J. Chem. Eng. Data 1981, 26, 277-279

Gas Solubilities of CO_2 in Heavy Hydrocarbons

Chien-Ping Chai and Michael E. Paulaitis*

Department of Chemical Engineering, University of Delaware, Newark, Delaware 19711

Gas solubilities at ambient pressures have been measured for CO_2 in *n*-hexadecane, *n*-eicosane, squalane, 1-methylnaphthalene, and quinoline over a temperature range from 298.6 to 330.2 K. The experimental data are analyzed by using the polymer solution theory of Flory to compare phase equilibrium behavior for paraffinic vs. aromatic solvents.

Introduction

Interest in solvent extraction with supercritical or near-critical fluids has been growing rapidly and in many applications has focused on CO_2 as the preferred solvent. Carbon dioxide is an attractive solvent primarily because it is inexpensive, readily available, and environmentally acceptable. Carbon dioxide also has a reasonable critical pressure (P_c = 72.86 atm) and a moderate critical temperature (T_c = 31.06 °C) which is important for applications involving heat-labile solutes. The high selectivity of CO_2 as a dense-gas or liquid solvent has been demonstrated experimentally (*1-3*), and supercritical CO_2 is currently used industrially as a selective solvent for decaffeinating coffee (*4*). At present, however, thermodynamic models for correlating and predicting the phase equilibrium behavior of dense-fluid mixtures containing simple hydrocarbons are not reliable for mixtures containing CO_2 and complex, heavy hydrocarbons—particularly aromatic hydrocarbons. Furthermore, experimental phase equilibrium data for such systems are scarce. As a preliminary study in our research program investigating the use of supercritical CO_2 for dense-fluid solvent extractions, we have measured the Henry's constants for CO_2 in various heavy hydrocarbon solvents at ambient temperatures and pressures. These solvents include *n*-hexadecane, *n*-eicosane, squalane, 1-methylnaphthalene, and quinoline.

Experimental Section

The experimental apparatus, shown in Figure 1, is similar to that used by Dymond and Hildebrand (*5*) and by Chappelow and Prausnitz (*6*) and consists of three elements: (1) the solvent reservoir and degassing flask (S), (2) the gas charging system (J and K), which is also used for pressure measurements, and (3) the thermostated equilibrium cell for contacting the gas and liquid solvent. The equilibrium cell consists of two bulbs, A (~100 mL) and B (~250 mL), connected directly by a capillary tube and by the side arm, C. The side arm contains a magnetically operated, metal-in-glass plunger for pumping solvent from B to A. The gas charging system consists of the gas buret, J, containing five bulbs ca. 10, 20, 40, 80, and 160 mL in volume, and the 100-mL graduated burette, K. The pressure within the system is balanced against atmospheric pressure transmitted through the open tube, L.

An experimental run begins by evacuating the entire apparatus. Solvent is then added through stopcock V15 and degassed by heating under vacuum for at least 2 h. With stopcock V18 closed, the degassed solvent is driven by its own vapor pressure onto bulb B until the meniscus is level with the mark b. The constant-temperature bath is then raised to the desired operating temperature, and excess solvent is removed through V17. The amount of solvent in the equilibrium cell is determined from the known volume of B (from the mark b to V16 and V17), and the solvent density measured at this temperature.

Carbon dioxide is added to the gas charging system through V9 with stopcocks V2, V8, V18, and V19 closed. The number of moles of CO_2 in the system is calculated from the calibrated volume of the burets—including the capillary tubing between V8, V9, V18, and V19—and the measured temperature and barometric pressure. The CO_2 is charged into bulb A by opening stopcock V18, and mixing of the two components is achieved by activating the plunger in side arm C. A reduction in pressure is observed at K as the gaseous solute dissolves in the solvent, and equilibrium is obtained when the mercury level in this buret remains constant. The number of moles of CO_2 adsorbed is determined by subtracting the calculated number of moles remaining in the vapor space (bulb A plus the gas charging system) from the total number of moles of CO_2 initially added to the system. The vapor pressure of the solvent is accounted for by using Antoine's equation (*7*). Henry's law constants are determined from the calculated solubility and the definition

$$H_{21} \equiv \lim_{x_2 \to 0} (f_2/x_2) \qquad (1)$$

where x_2 is the mole fraction of CO_2 in the liquid phase and f_2 is the fugacity of CO_2, determined from its partial pressure.

The bath temperature is then lowered to the next desired value, and the procedure is repeated. The volume now occupied by the solvent is recalculated by knowing the initial charge of solvent and the measured solvent density at the new temperature. The vapor space volume at this temperature is adjusted accordingly.

Carbon dioxide ("bone dry") is supplied by Linde, and the solvents are Fisher certified grade obtained from Fisher Scientific Co. The purity of each solvent is verified by gas-chromatographic analysis and subsequently used without further purification.

Results

The experimental Henry's constants at various temperatures are given in Table I and plotted in Figure 2. Each tabulated value represents the result of an independent experimental determination, and, as indicated in Table I, the reproducibility is generally better than 1%. The results plotted in Figure 2 show that, over the limited temperature range investigated, the logarithm of the Henry's constant is essentially linear with temperature for each solvent studied. Our experimental results for CO_2–eicosane and CO_2–*n*-hexadecane are compared with those of Huie, Luks, and Kohn (*1*) and Tremper and Prausnitz (*8*), respectively, and the agreement is shown to be excellent. For CO_2–1-methylnaphthalene, the Henry's constant at 300 K obtained in this work is 153.8 atm, which agrees very well with the value of 151 atm obtained by Horvath, Sebastian, and Chao (*9*) but is appreciably higher than the value of 127.0 atm reported by Tremper and Prausnitz (*8*).

The experimental data can be interpreted by using the correlation for gas solubilities suggested by Chappelow and Prausnitz (*6*) which is based upon the polymer solution theory of Flory (*8*). An expression for the Henry's constant is obtained by considering the dissolution of gaseous CO_2 into the liquid solvent as a two-step process: (1) condensation of the pure,

0021-9568/81/1726-0277$01.25/0

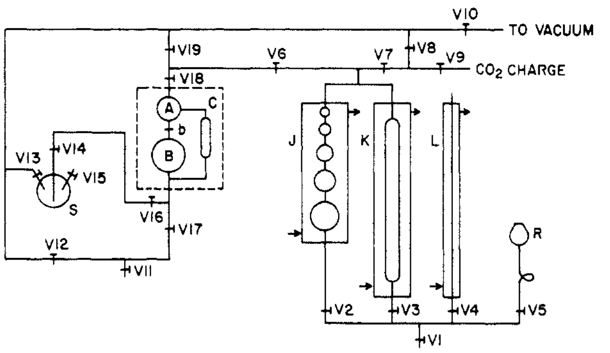

Figure 1. Schematic diagram of the experimental apparatus for measuring gas solubilities.

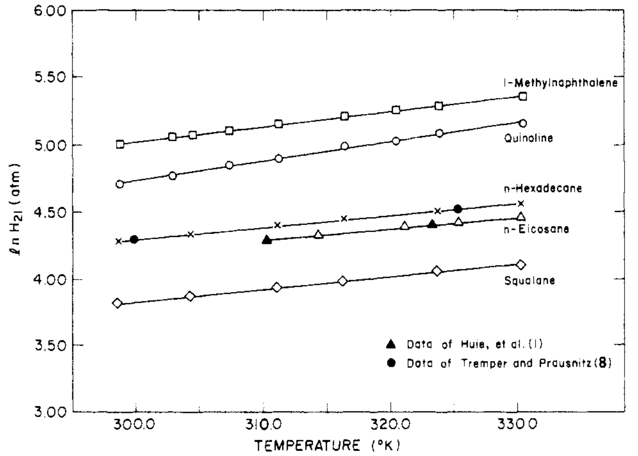

Figure 2. Experimental Henry's constants for CO_2 in various heavy hydrocarbons obtained in this work.

ideal gas at 1-atm partial pressure to the pure liquid and (2) mixing the pure hypothetical liquid with the solvent. Thus

$$H_{21} = \gamma_2^{\infty} f_2^{0L} \qquad (2)$$

where γ_2^{∞} is the infinite-dilution activity coefficient of hypothetical liquid CO_2 in the solvent and f_2^{0L} is the pure-component fugacity of hypothetical liquid CO_2. The generalized correlation of Prausnitz and Chueh (11) is extrapolated to reduced temperatures of 0.98–1.10 to obtain f_2^{0L}. Following Flory (10), the infinite-dilution activity coefficient is conveniently divided into two terms:

$$\ln \gamma_2^{\infty} = \ln \gamma_2^{c} + \chi \qquad (3)$$

The first term on the right represents the combinatorial contribution to γ_2^{∞}, which is obtained from the configurational entropy of mixing given by Staverman (12). The empirical parameter χ (i.e., the Flory parameter) represents the residual contribution to γ_2^{∞} comprising contributions due to (1) differences in liquid-state properties of the solute and solvent (i.e., equation-of-state or free-volume contributions) and (2) intermolecular-force interactions (i.e., lattice-theory interchange energies). The Flory parameter is usually divided into enthalpic (subscript H) and entropic (subscript S) parts

$$\chi = \chi_H + \chi_S \qquad (4)$$

using the Gibbs–Helmholtz relations

$$\chi_H = \Delta \bar{h}_2^{R}/(RT) = -T(\partial \chi/\partial T) \qquad (5)$$

$$\chi_S = -\Delta \bar{s}_2^{R}/R = (\partial \chi T/\partial T) \qquad (6)$$

where $\Delta \bar{h}_2^{R}$ and $\Delta \bar{s}_2^{R}$ are the partial molar residual enthalpy and entropy of mixing, respectively.

Experimental Henry's constants for a particular solvent and calculated values of f_2^{0L} are used in eq 2 to obtain γ_2^{∞} over the temperature range investigated. The temperature-independent $\ln \gamma_2^{c}$ is determined by following procedures outlined in Chappelow and Prausnitz (6) and used in eq 3 with the calculated values of γ_2^{∞} to give χ as a function of temperature. The parameters χ_H and χ_S are subsequently obtained from eq 4–6. The calculated results are presented in Table II for each of the five solvents studied. These results must be considered semiquantitative at best because of the limited temperature range studied as well as the rudimentary nature of the solution theory employed. However, several important conclusions can be drawn from the analysis.

Comparison of calculated results for the paraffinic solvents and 1-methylnaphthalene indicates that the combinatorial contribution to H_{21} is greater for the long-chain hydrocarbons than for the aromatic solvent, as expected, while the total residual contribution is nearly the same in all cases. For *n*-hexadecane, *n*-eicosane, and squalane, neither χ_H nor χ_S differs appreciably from one solvent to another. However for 1-methylnaphthalene,

Table I. Experimental Henry's Constants for Carbon Dioxide in Heavy Hydrocarbons

T, K	H_{21}, atm	T, K	H_{21}, atm
	Solvent: *n*-Hexadecane		
298.6	71.42	316.2	84.57
298.6	71.92	316.2	85.66
304.3	75.78	323.6	89.46
304.3	75.98	323.6	91.13
311.0	80.77	330.2	95.11
311.0	81.40	330.2	95.47
	Solvent: Squalane		
298.6	45.35	316.2	53.92
298.6	44.92	316.2	53.22
304.3	48.16	323.6	57.85
304.3	47.75	323.6	57.56
311.0	51.33	330.2	60.43
311.0	50.94		
	Solvent: *n*-Eicosane		
314.3	75.58	325.3	82.75
321.0	80.62	330.2	86.20
321.0	80.24	330.2	86.21
325.3	83.03		
	Solvent: 1-Methylnaphthalene		
298.6	147.75	316.2	180.78
298.6	149.80	316.2	183.29
298.6	149.24	316.2	181.10
302.7	157.04	320.2	191.32
304.3	159.32	323.6	194.79
307.1	163.75	323.6	198.42
307.1	165.48	323.6	195.13
307.1	164.18	330.2	210.85
311.0	172.37		
	Solvent: Quinoline		
298.6	110.51	316.2	146.97
298.6	111.66	316.2	144.79
302.7	118.36	320.2	153.72
302.7	117.17	320.2	151.20
302.7	118.09	320.2	152.81
307.1	127.15	323.6	160.83
307.1	128.68	323.6	162.81
311.0	134.52	323.6	160.03
311.0	133.06	330.2	172.07
311.0	134.57		
316.2	144.74		

Table II. Calculated Values of $\ln \gamma_2^{c}$, χ_H, and χ_S for Carbon Dioxide in the Solvents Studied

solvent	$\ln \gamma_2^{c}$	χ_H	χ_S
n-hexadecane	−1.27	0.70	1.20
n-eicosane	−1.46	0.58	1.40
squalane	−1.82	0.62	1.37
1-methylnaphthlane	−0.59	0.18	1.78
quinoline	−0.39	−0.88	2.36

χ_S is significantly more positive, and χ_H less so. The asymmetry of χ_H and χ_S is even more dramatic for quinoline. Flory (*10*) has shown that χ_S is determined predominantly by equation-of-state contributions; χ_H also consists primarily of these contributions when the mixture species are similar in molecular nature. The effect of such contributions is to increase χ_S and decrease χ_H. Therefore our results show that differences in liquid-state properties become more important for CO_2–aromatic hydrocarbon mixtures compared to CO_2–alkane mixtures.

The significant decrease in χ_H noted here for 1-methylnaphthalene compared to values for the paraffinic solvents is not observed for gas solubilities of simple hydrocarbon gases (CH_4, C_2H_6, and C_3H_8) in these solvents (*6*). In fact, for these gases, χ_H becomes somewhat more positive when the solvent is 1-methylnaphthalene. This suggests that intermolecular-force interactions are more important for CO_2 in the aromatic solvent. The decrease in χ_H observed for this system implies that CO_2–1-methylnaphthalene solutions exhibit solvation effects. The CO_2–quinoline system with a negative χ_H exhibits stronger solvation effects, as expected. Therefore, in modeling the phase equilibrium behavior of mixtures containing CO_2 and complex aromatic hydrocarbons, consideration must be given to increased importance of both these solvation effects and effects due to differences in liquid-state properties of CO_2 and the aromatic constituent.

Acknowledgment

We are grateful to Stan Sandler, who gave us permission to use his experimental equipment as well as modify it for our particular experiments.

Glossary

f	fugacity
H_{21}	Henry's law constant for solute 2 in solvent 1
R	gas constant
T	absolute temperature
x	liquid-phase mole fraction
$\Delta\bar{h}^R$	partial molar residual enthalpy of mixing
$\Delta\bar{s}^R$	partial molar residual entropy of mixing

Greek Letters

γ	activity coefficient
χ	Flory parameter
χ_H	enthalpic part of the Flory parameter
χ_S	entropic part of the Flory parameter

Subscripts

1	solvent
2	solute

Superscripts

c	combinatorial
OL	pure liquid phase
∞	infinite dilution

Literature Cited

(1) Huie, N. C.; Luks, K. D.; Kohn, J. P. *J. Chem. Eng. Data* **1973**, *18*, 311.
(2) Kulkarni, A. A.; Luks, K. D.; Kohn, J. P. *J. Chem. Eng. Data* **1974**, *19*, 349.
(3) Francis, A. W. *J. Phys. Chem.* **1954**, *58*, 1099.
(4) Vitzthum, O.; Hubert, P. German Patent 2 357 590, 1975.
(5) Dymond, J.; Hildebrand, J. H. *Ind. Eng. Chem. Fundam.* **1967**, *6*, 130.
(6) Chappelow, C. C.; Prausnitz, J. M. *AIChE. J.* **1974**, *20*, 1097.
(7) Reid, R. C.; Prausnitz, J. M.; Sherwood, T. K. "The Properties of Gases and Liquids", 3rd ed.; McGraw-Hill: New York, 1977; Appendix A.
(8) Tremper, K. K.; Prausnitz, J. M. *J. Chem. Eng. Data* **1976**, *21*, 295.
(9) Horvath, M. J.; Sebastian, H. M.; Chao, K. C. *Ind. Eng. Chem. Fundam.*, in press.
(10) Flory, P. J. *Discuss. Faraday Soc.* **1970**, *50*, 7.
(11) Prausnitz, J. M.; Chueh, P. L. "Computer Calculations for High-Pressure Vapor–Liquid Equilibria"; Prentice-Hall: Englewood Cliffs, NJ, 1968.
(12) Staverman, A. J. *Recl. Trav. Chim. Pays-Bas* **1950**, *69*, 163.

Received for review September 12, 1980. Accepted December 5, 1980.

Solubility of Carbon Dioxide in Molten Alkali Halides and Nitrates and Their Binary Mixtures

Eizo Sada,* Shigeo Katoh, Hidehumi Yoshii, Ikuo Takemoto, and Naofumi Shiomi
Chemical Engineering Department, Kyoto University, Kyoto 606, Japan

The solubilities of carbon dioxide in molten alkali halides and nitrates and their binary mixtures were determined at 1 atm by the elution method. The solubility values predicted by the Blander model showed fairly good agreement with the experimental values for alkali halides but were far lower than the experimental values for alkali nitrates. Linear relations between the mole fraction of the salts and the logarithm of the Henry's-law constants of the gas were observed in binary mixtures of $NaNO_3$–$RbNO_3$ and NaCl–KCl.

In investigating the kinetics of gas–molten salt reactions, it is necessary to measure solubilities of gases in molten salts. The solubility data of nonpolar gases, such as He, Ar, N_2 and O_2, have been reported (*3*, *4*). Little is known, however, about solubilities of polar or triatomic gases in pure molten slats and their mixtures (*2*, *7*, *9*). In the previous work (*8*), solubilities of carbon dioxide in four molten salts were measured by a simplified elution method. In the present work, solubilities of carbon dioxide in pure alkali halides and nitrates and their binary mixtures, which are widely used as reaction media in gas–molten salt systems, were determined at 1 atm by the same elution method as part of a systematic investigation of the solubility of gas in molten salts. The alkali halides and nitrates used were NaCl, KCl, RbCl, KBr, $LiNO_3$, $NaNO_3$, KNO_3, $RbNO_3$, and $CsNO_3$, and the binary systems were $NaNO_3$–$LiNO_3$, $NaNO_3$–$RbNO_3$, and NaCl–KCl.

Experimental Section

The experimental apparatus and procedure are essentially as described in the previous paper (*8*). The absorption and elution chamber used in this work was made of quartz glass and was 13 mm in inside diameter and 48 mm in height. The gas inlet, the gas outlet, and the bubbling tube attached to the chamber were also made of quartz glass. The temperature of the chamber was kept constant within ±1 °C.

The binary mixtures were prepared by weighing the two salts and then melting them in a chamber at a temperature which